METROLOGICAL CHARACTERIZATION OF OPTICAL 3D COORDINATE MEASUREMENT SYSTEMS - COMPARISON OF ALTERNATIVE HARDWARE DESIGNS AS PER ISO 10360

Davide M. Fabris*[1], Paolo Brambilla[1], Chiara Conese[1], Marino M. Maspes[2], R. Sala[1], M. Tarabini[1]

[1] Politecnico di Milano, Mechanical Engineering Department, Via La Masa 1, 20156 Milan, Italy
[2] Politecnico di Milano, School of Electronics, Information and Bioengineering, Via Ponzio 34, 20133 Milan, Italy

Technical Commission II

KEY WORDS: 3D Vision, 3D Scanner Metrology, ISO 10360-13, Structured Light, Metrological Characterization.

ABSTRACT:

This research focuses on the characterization of the metrology of Optical 3D Coordinate Measurement Systems (O3DCMS). The focus is set on the identification and execution of the procedure indicated by the currently active technical standards related to industrial O3DCMS, for their metrological assessment, objective comparison, and performance tracking. This work leads to the implementation of an ad hoc software for the execution of the standard tests by the ISO 10360-13 standard. The implemented software application is employed in a real-case scenario for evaluating the performances of an industrial 3D scanner based on structured light. The specific hardware components to be assessed are two light sources of the active stereoscopic vision system, named Digital Light Projectors (DLP). The case study applies the procedures and metrics indicated by the active standards to objectively compare two alternative hardware design of the system under test. This results in the identification of the most performing hardware configuration, allowing the selection of the best system design, basing on objective metrological parameters.

1. INTRODUCTION

This work is motivated by the necessity for the identification of a unique procedure for the evaluation of O3DCMS. Moreover, the need for the implementation of a software for executing the Optical 3D Metrology (O3DM) characterization was expressed by Innovative Security Solutions s.r.l., a producer of industrial 3D scanners for robotic bin-picking. A systematic literature review was conducted, obtaining an overview of the scientific production in the O3DM field (Beraldin et al., 2015; Carfagni et al., 2017; Giancola et al., 2018; Hodgson et al., 2017; Luhmann & Wendt, 2000; Servi et al., 2008, 2021). The focus was then also set on the identification of technical standards used to perform an objective metrological characterization of O3DCMS (ISO, 2021; VDI/VDE, 2012). Moreover, a list of the most commonly used artifacts was gathered (Acko et al., 2012; Eiríksson et al., 2016; Guidi, 2013; Hess et al., 2014; McCarthy et al., 2011; Mendricky & Sobotka, 2020), see Figure 1.

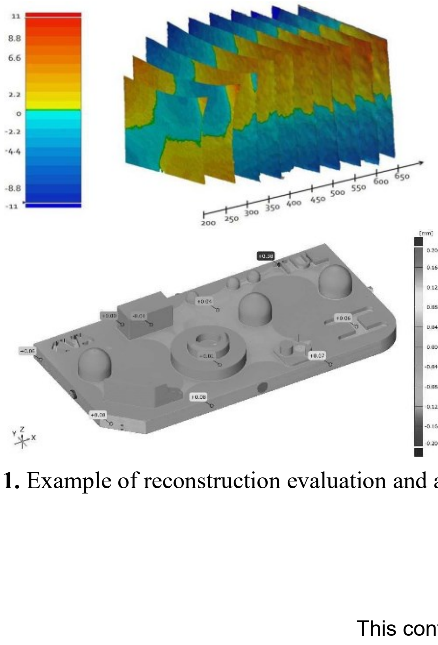

Figure 1. Example of reconstruction evaluation and artifacts.

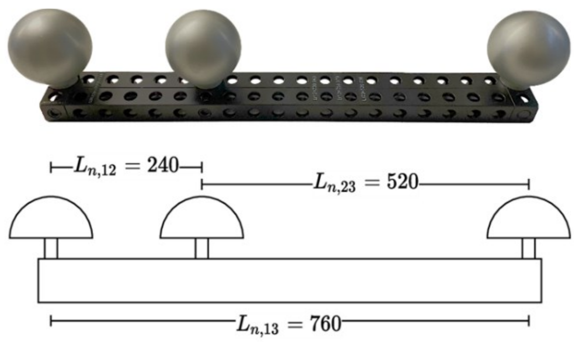

Figure 2. The ball-bar artifact used for the characterization of the O3DCMS. Nominal dimensions are reported in millimetres, spheres feature 120 mm diameters.

In general, O3DCMS can be classified in three categories (Beraldin et al., 2015; Faugeras, 1993; Giancola et al., 2018; Huang & Zhang, 2006; Luhmann, 2010) depending on their working distance, namely nano/micro, close, and mid-to-long ranges. In the field of industrial engineering, the majority of these devices operate in the close range, i.e., from 10 mm to 2 m. Past and currently active standards (ISO, 2021; ISO/IEC, 2012; VDI/VDE, 2008, 2012) specify the quantitative parameters to be measured for expressing the metrological performances of O3DCMS. The parameters must be evaluated with calibrated artifacts, such as the aluminium ball-bar in Figure 2. The characterization procedure may be performed also to identify the effect of influencing factors. Among others, the most significant ones are the scanning parameters, the target material, the surface finishing, and the scene illumination.

The methodology for performing the metrological characterization of O3DCMS defined by the standards was implemented in a software and employed in an industrial case scenario. Specifically, the application of the standardized procedure allowed the comparison of two solutions, objectively analysing metrology and identifying the best performing design.

This contribution has been peer-reviewed.
https://doi.org/10.5194/isprs-archives-XLVIII-2-W2-2022-39-2022

Figure 3. Setup used during the execution of the tests on the 3DCPS Fast scanner. The device, the robot used for the calibration, and the ball-bar artifact are shown.

The paper is structured as follows. Section 2 reports the method followed for the implementation and the execution of the testing procedure indicated by the ISO standards. Section 3 focuses on the obtained results, providing valuable insights. Section 4 is related to the discussions and conclusions.

2. METHOD

The System Under Test (SUT) is the 3D CPS Fast (Figure 3), a 3D scanner engineered by Innovative Security Solutions s.r.l. for robotic bin-picking. The system is equipped with two industrial cameras and a DLP. Via structured light (Gu et al., 2014; S. Zhang, 2013; Y. Zhang & Yilmaz, 2016), the device can relate the deformation of projected light patterns to the 3D shape of the objects in the measurement volume. Experiments consisted in the comparison of the performances of the SUT while mounting two different DLPs, named DLP4500 and DLP4750. Prior to testing, each device underwent optical calibration (Li, 2008; Z. Zhang, 2000) at a working distance of 1000 mm, with a depth of field from 900 to 1100 mm. The horizontal and vertical ranges of measurement of the devices are 600 mm and 400 mm. The repeatability of the optical calibration was ensured by harnessing a Stäubli TX-60 robot for the displacement of the calibration board, as shown in Figure 4.

Figure 4. Robotic setup used for the calibration of the O3DCMS. The same 3D poses of the calibration board were used while calibrating both devices to grant repeatability.

A ball-bar artifact composed by three rigidly connected spheres was used for conducting the experiments, its nominal dimensions are indicated in Figure 2. The primary measurement of the spheres' diameters and distance were evaluated by means of a Coordinate Measurement Machine at a Hexagon Metrology Intelligence facility, they are reported in Table 1. In accordance with the ISO 10360-13 (ISO, 2021) standard, the spheres featured a diffusely reflecting surface. The only spheres considered for the qualification of the O3DCMS are the two on the left in Figure 2. The scene light intensity level was measured with a luxmeter, its value was constantly among 700 and 900 lux.

	Primary Measurement	
Quantity	Value	Unit
Diameter - Sphere 1	119.981	mm
Diameter - Sphere 2	119.985	mm
Distance - Sphere 1,2	239.980	mm

Table 1. Primary measurements of the ball-bar artifact obtained by a CMM at Hexagon Metrology Intelligence.

As per the ISO 10360-13 standard, the artifact was displaced in the working volume to reach the 3D poses reported in Figure 5. In each position, the artifact was scanned three times to assess the measurement repeatability and to grant generality. The acquired data were then processed by means of the developed software. The spherical objects were detected in the pointclouds through the min-squares formulation of the identification problem, as reported in the next equations. The analytical form of a sphere is:

$$(x - x_c)^2 + (y - y_c)^2 + (z - z_c)^2 = r^2 \quad (1)$$

For each i-th point of the N belonging to a spherical pointcloud:

$$x_i^2 + y_i^2 + z_i^2 - 2\,(xx_c + yy_c + zz_c) + x_c^2 + \\ + y_c^2 + z_c^2 = r^2 \quad (2)$$

Rewriting in matrix form, the following matrices are defined:

$$[\boldsymbol{A}]_{Nx4} = \begin{bmatrix} x_1 & y_1 & z_1 & 1 \\ x_2 & y_2 & z_2 & 1 \\ \vdots & \vdots & \vdots & \vdots \\ x_N & y_N & z_N & 1 \end{bmatrix}_{Nx4} \quad (3)$$

$$[\boldsymbol{b}]_{Nx1} = \begin{bmatrix} x_1^2 + y_1^2 + z_1^2 \\ x_2^2 + y_2^2 + z_2^2 \\ \vdots \\ x_N^2 + y_N^2 + z_N^2 \end{bmatrix}_{Nx1} \quad (4)$$

$$[\boldsymbol{x}]_{4x1} = \begin{bmatrix} 2x_c \\ 2y_c \\ 2z_c \\ x_c^2 + y_c^2 + z_c^2 - r^2 \end{bmatrix}_{4x1} \quad (5)$$

The over-determined linear system of equations can then be rewritten as reported in Equation 6. It can be solved by minimizing the L2-norm of $\boldsymbol{b} - A\hat{\boldsymbol{x}}$, obtaining the least-squares solution $\hat{\boldsymbol{x}}$, from which the unknowns can be derived.

$$\hat{\boldsymbol{x}}_{4x1} = A^{-1}\boldsymbol{b} \quad \leftarrow \quad \min(\|\boldsymbol{b} - A\hat{\boldsymbol{x}}\|_2) \quad (6)$$

where: x_i, y_i, z_i are the i-th point coordinates,
x_c, y_c, z_c are the centre of the sphere coordinates,
r is the radius of the sphere,
$\hat{\boldsymbol{x}}$ is the least-squares problem solution.

This contribution has been peer-reviewed.
https://doi.org/10.5194/isprs-archives-XLVIII-2-W2-2022-39-2022

Position	Sphere 1 in voxel	Sphere 2 in voxel
1	1	7
2	4	6
3	5	3
4	8	2
5	2	4
6	3	1
7	3	4
8	6	8
9	7	5
10	6	5
11	4	5
12	3	6

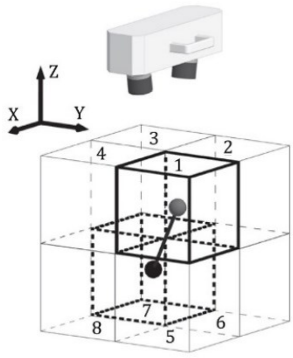

Figure 5. On the left the table with the poses to be reached by ball-bar artifact. On the right the first pose of the ball-bar.

The probing form dispersion error (P_F, Figure 6), the probing size error (P_S, Figure 7), and the distortion error (D_{CC}) indicated by the ISO 10360-13 were then computed. The P_F is the width of the spherical shell that encompasses a designated percentile (i.e., 95%) of all measured points on the spherical surfaces. The P_S is the difference between the measured diameters of the test spheres and their calibrated values. The D_{CC} is the difference between the measured and calibrated values of the spheres' centre-to-centre distances. Each parameter is averaged over the poses indicated by the standard. Respectively, the P_F and the P_S relate to the accuracy and the precision of the spheres' diameters measurement, while the D_{CC} highlights the accuracy in the spheres' centre-to-centre distance measurement.

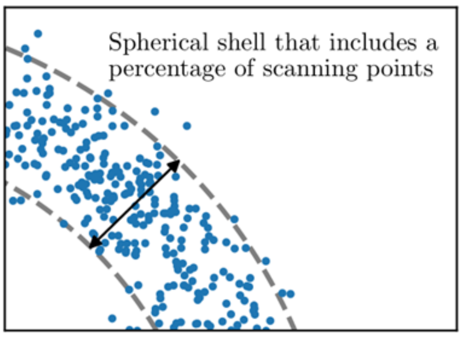

Figure 6. Graphical representation of the probing form dispersion error (P_F). The two dashed lines represent the 95% confidence interval used for the computation of the parameter.

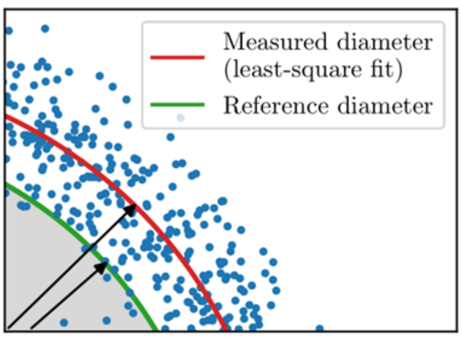

Figure 7. Graphical representation of the probing size error (P_S). The green circle identifies the primary value of the sphere diameter, the red circle identifies the fitted sphere diameter.

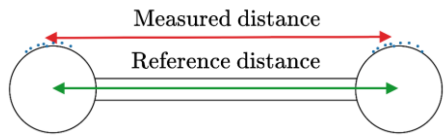

Figure 8. Graphical representation of the Distortion Error (D_{CC}). The parameter is defined as the absolute value of the difference between the measured and reference diameters.

An ad hoc software was developed to implement the procedure reported by the ISO 10360-13 standard. Coupling MVTec HALCON and Python, the software first allows to sub-sample the raw 3D data. Then the scattered noise is filtered with a density-based filter. The resulting scan is processed to identify and cluster the spheres within the scene. The least-squares fitting is applied to each spherical object. Eventually the required parameters are computed. The entire workflow of the application is shown in Figure 9. The resulting software was employed for assessing the two alternative hardware configurations of the 3D CPS Fast scanner.

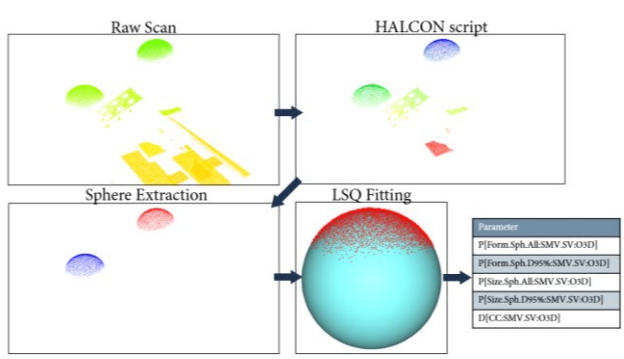

Figure 9. Schematic representation of the workflow of the developed software for the execution of the ISO10360-13 standard. The raw scan is sub-sampled, and noise is removed by a density-based filter. The spherical objects are clustered, and the least squares fitting is operated, eventually the ISO 10360-13 parameters are computed.

3. RESULTS

Table 2 and Figure 10 report the results of the comparison of the two alternative designs of the 3D CPS Fast. Parameters are reported in the worst of the three repetitions for each position, both in absolute and relative terms, with respect to the corresponding primary measurement. DLP4750 features higher accuracy and precision in the reconstruction of spherical surfaces, as testified by P_F and P_S. The D_{CC} parameter testifies a higher accuracy of DLP4750 in centre-to-centre distance measurement.

	ISO Parameters		
Quantity	DLP4500	DLP4750	Unit
Probing Form Error (P_F)	1.89	1.57	mm
Probing Size Error (P_S)	0.62 (0.5%)	0.51 (0.4%)	mm
Distortion Error (D_{CC})	0.76 (0.3%)	0.69 (0.3%)	mm

Table 2. Resulting parameters from the ISO 10360-13 Tests. First column refers to DLP4500, second column to DLP4750.

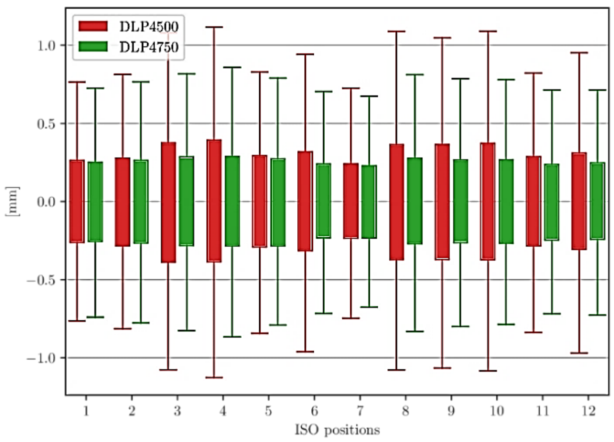

Figure 10. Box plot representing the obtained results in terms of Probing Form Error P_F parameters for the DLP4500 (red) and the DLP4500 (green).

4. DISCUSSION AND CONCLUSIONS

The methodology for performing the metrological characterization of O3DCMS by the ISO 10360-13 standards was investigated, implemented, and evaluated in a real case scenario. The tested device was the 3D CPS Fast, an industrial 3D scanner engineered by Innovative Security Solutions s.r.l., in two of its alternative hardware designs. The application of the standardized procedure allowed the objective comparison of the two solutions, highlighting their performances in terms of O3DM.

As evidenced by Table 2 and Figure 10, the introduction of the DLP4750 leads to an enhancement of the metrological performances of the device. The amelioration is testified by every parameter specified by the ISO 10360-13 standard. Namely, the Probing Form Error is reduced by 17%, the Probing Size Error is reduced by 15%, the Distortion Error is reduced by 9%. The DLP4750 results thus being the most performing DLP.

Future works involve the evaluation of the influence of the material, surface finishing and scene illumination on the parameters defined by the ISO 10360-13 technical standard.

ACKNOWLEDGEMENTS

Authors acknowledge Innovative Security Solutions s.r.l. for granting the possibility to conduct the experimental study on their 3D scanner, the 3D CPS Fast, through the robotic setup. Authors would also like to acknowledge Hexagon Manufacturing Intelligence for granting the use their CMMs and 3D scanners for the retrieval of the primary measurements of the ball-bar.

REFERENCES

Acko, B., McCarthy, M., Haertig, F., & Buchmeister, B. (2012). Standards for testing freeform measurement capability of optical and tactile coordinate measuring machines. *Measurement Science and Technology*, *23*(9). https://doi.org/10.1088/0957-0233/23/9/094013

Beraldin, J.-A., Mackinnon, D., & Cournoyer, L. (2015). Metrological characterization of 3D imaging systems: progress report on standards developments. In B. Larquier (Ed.), *17th International Congress of Metrology*. EDP Sciences. https://doi.org/10.1051/metrology/20150013003

Carfagni, M., Furferi, R., Governi, L., Servi, M., Uccheddu, F., & Volpe, Y. (2017). On the Performance of the Intel SR300 Depth Camera: Metrological and Critical Characterization. *IEEE SENSORS JOURNAL*, *17*(14). https://doi.org/10.1109/JSEN.2017.2703829

Eiríksson, E. R., Wilm, J., Pedersen, D. B., & Aanæs, H. (2016). Precision and accuracy parameters in structured light 3-d scanning. *The International Archives of the Photogrammetry, Remote Sensing and Spatial Information Sciences*, *XL-5/W8*. https://doi.org/10.5194/isprs-archives-xl-5-w8-7-2016

Faugeras, O. (1993). *Three-Dimensional Computer Vision*. The MIT Press.

Giancola, S., Valenti, M., & Sala, R. (2018). A survey on 3D cameras: Metrological comparison of time-of-flight, structured-light and active stereoscopy technologies. In *Springer Briefs in Computer Science*. https://doi.org/10.1007/978-3-319-91761-0

Gu, Q., Herakleous, K., & Poullis, C. (2014). *3DUNDERWORLD-SLS: An Open-Source Structured-Light Scanning System for Rapid Geometry Acquisition*. 1–30.

Guidi, G. (2013). Metrological characterization of 3D imaging devices. *Videometrics, Range Imaging, and Applications XII; and Automated Visual Inspection*, *8791*(May 2013), 87910M. https://doi.org/10.1117/12.2021037

Hess, M., Robson, S., & Hosseininaveh Ahmadabadian, A. (2014). A contest of sensors in close range 3D imaging: Performance evaluation with a new metric test object. *International Archives of the Photogrammetry, Remote Sensing and Spatial Information Sciences - ISPRS Archives*, *40*(5), 277–284. https://doi.org/10.5194/isprsarchives-XL-5-277-2014

Hodgson, J. R., Kinnell, P., Justham, L., Lohse, N., & Jackson, M. R. (2017). Novel metrics and methodology for the characterization of 3D imaging systems. *Optics and Lasers in Engineering*, *91*, 169–177. https://doi.org/10.1016/j.optlaseng.2016.11.007

Huang, P. S., & Zhang, S. (2006). Novel method for structured light system calibration. *Optical Engineering*, *45*(8), 083601. https://doi.org/10.1117/1.2336196

ISO. (2021). *BSI Standards Publication Geometrical product specifications (GPS) — Acceptance and reverification tests for coordinate measuring systems (CMS) Part 13: Optical 3D CMS.*

ISO/IEC. (2012). *GUIDE 98-3:2008(E) - Uncertainty of measurement - Part 3 : Guide to the expression of uncertainty in measurement*.

Li, Z. (2008). Accurate calibration method for a structured light system. *Optical Engineering*, *47*(5), 053604. https://doi.org/10.1117/1.2931517

Luhmann, T. (2010). Close range photogrammetry for industrial applications. *ISPRS Journal of Photogrammetry and Remote Sensing*, *65*(6), 558–569. https://doi.org/10.1016/J.ISPRSJPRS.2010.06.003

Luhmann, T., & Wendt, K. (2000). *Recommendations for an acceptance and verification test of optical 3-D measurement systems*. https://www.researchgate.net/publication/228918599

McCarthy, M. B., Brown, S. B., Evenden, A., & Robinson, A. D. (2011). NPL freeform artefact for verification of non-contact measuring systems. *Three-Dimensional Imaging, Interaction, and Measurement*, *7864*, 78640K. https://doi.org/10.1117/12.876705

Mendricky, R., & Sobotka, J. (2020). Accuracy Comparison of the Optical 3D Scanner and CT Scanner. *Manufacturing Technology*, *20*(6), 791–801. https://doi.org/10.21062/MFT.2020.120

Servi, M., Buonamici, F., Luca Puggelli, ·, & Volpe, Y. (2008). New metrological characterization strategy for 3D multi-camera systems. *International Journal on Interactive Design and Manufacturing (IJIDeM)*, *15*, 69–72. https://doi.org/10.1007/s12008-020-00721-5

Servi, M., Buonamici, F., Luca Puggelli, ·, & Volpe, Y. (2021). A new metrological characterization strategy for 3D multi-camera systems. *International Journal on Interactive Design and Manufacturing (IJIDeM)*, *15*, 69–72. https://doi.org/10.1007/s12008-020-00721-5

VDI/VDE. (2008). *Optical 3D-measuring systems Multiple view systems based on area scanning VDI/VDE 2634 Part 3*. www.vdi-richtlinien.de

VDI/VDE. (2012). *Optical 3D-measuring systems Optical systems based on area scanning VDI/VDE 2634 Part 2*. www.vdi-richtlinien.de

Zhang, S. (2013). Handbook of 3D Machine Vision. In *Series in optics and optoelectronics*.

Zhang, Y., & Yilmaz, A. (2016). Structured light based 3D scanning for specular surface by the combination of gray code and phase shifting. *International Archives of the Photogrammetry, Remote Sensing and Spatial Information Sciences - ISPRS Archives*, *41*(July), 137–142. https://doi.org/10.5194/isprsarchives-XLI-B3-137-2016

Zhang, Z. (2000). A Flexible New Technique for Camera Calibration. *IEEE Transactions on Pattern Analysis and Machine Intelligence*, *22*(11), 1330–1334.